NISTIR 5136

# Dose in Water from External Irradiation by Electrons: Radiation Protection Data

**Stephen M. Seltzer**

U.S. DEPARTMENT OF COMMERCE
Technology Administration
National Institute of Standards and Technology
Physics Laboratory
Ionizing Radiation Division
Gaithersburg, MD 20899

Prepared for:

U.S. Department of Energy
Office of Health
and Environmental Research
Washington, D.C. 20585

NISTIR 5136

# Dose in Water from External Irradiation by Electrons: Radiation Protection Data

**Stephen M. Seltzer**

U.S. DEPARTMENT OF COMMERCE
Technology Administration
National Institute of Standards
and Technology
Gaithersburg, MD 20899

Prepared for:

U.S. Department of Energy
Office of Health and Environmental Research
Washington, D.C. 20585

February 1993


**U.S. DEPARTMENT OF COMMERCE**
**Ronald H. Brown, Secretary**

**NATIONAL INSTITUTE OF STANDARDS**
**AND TECHNOLOGY**
**Raymond G. Kammer, Acting Director**

# Dose in Water from External Irradiation by Electrons: Radiation Protection Data[1]

Stephen M. Seltzer
Ionizing Radiation Division
National Institute of Standards and Technology[2]
Gaithersburg, MD 20899

Abstract

Results from electron Monte Carlo calculations are given for the absorbed dose at depths of 7, 40, 300 and 1000 mg/cm$^2$ in a slab water phantom irradiated by electrons incident with kinetic energies from 50 keV to 10 MeV and at angles (with respect to the normal to the surface) of 0, 15, 30, 45, 60, 75 and 89°. Electron number and energy reflection coefficients are given also for these cases.

## I. Introduction

This report presents results of electron Monte Carlo calculations performed to obtain the absorbed dose from monoenergetic, monodirectional electron irradiation of a water phantom. The calculations were prompted by a request [1][3] by a task group representing the International Commission on Radiation Protection (ICRP) and the International Commission on Radiation Units and Measurements (ICRU), whose aim is the compilation of up-to-date data for neutrons, photons and electrons to provide for conversion factors between field quantities and operational quantities used in radiation protection.

The calculations reported here concern only electron irradiation, and were used to obtain the absorbed dose at depths $d$ of 7, 40, 300 and 1000 mg/cm$^2$, for angles of incidence $\alpha$ (with respect to the normal to the surface of a slab phantom) of 0, 15, 30, 45, 60, 75 and 89°, and for electrons with energies of 10, 7, 4, 3, 2, 1.5, 1, 0.8, 0.7, 0.6, 0.4, 0.2, 0.1, 0.09, 0.08, 0.07, 0.06 and 0.05 MeV incident on a slab water phantom. Because the quality factor is accepted as unity for electrons, there is no difference between dose equivalent and absorbed dose in these cases. Therefore, the results correspond to the *personal dose equivalent* $H_p(d)$ as defined by the ICRU [2] and the ICRP [3]. An analogous quantity is the *directional dose equivalent* $H'(d,\alpha)$, but is defined for the ICRU sphere.[4] At the lower energies and smaller angles, the slab and sphere results should be nearly the same. However, to avoid any possible confusion, we report our results as $H_p(d,\alpha)$, where the explicit dependence on $\alpha$ has been added to the notation in the same manner as done in section A.4 of reference [2].

---

[1]Work supported by the U.S. Department of Energy, Office of Health and Environmental Research.

[2]Physics Laboratory, Technology Administration, U.S. Department of Commerce.

[3]Figures in brackets indicate literature references at the end of this paper.

[4]The ICRU sphere is a 30-cm diameter sphere of tissue-equivalent material (76.2% O, 11.1% C, 10.1% H, and 2.6% N, by weight) with a density of 1 g/cm$^3$.

In the interest of making these results available in a timely fashion, this report will be brief. Some salient features of the Monte Carlo model are given in Section II, and the results are discussed in Section III.

## II. Monte Carlo Model

The calculations were performed using the ETRAN code [4], which also serves as the basis for the more general-geometry codes in the latest Integrated Tiger Series, ITS-3.0 [5]. A more complete discussion of the current Monte Carlo model can be found in [4]. The electron trajectories are schematized as series of short path segments[5] for which the net collision energy losses and net angular deflections are sampled from multiple-scattering distributions. The collision energy loss is sampled from the Landau distribution [6], truncated [7] so as to yield a mean collision energy loss consistent with the stopping powers given in ICRU Report 37 [8], and convoluted with the Blunck-Leisegang correction [9] with semi-empirical modifications [4]. Angular deflections are sampled from the Goudsmit-Saunderson multiple-scattering distribution [10], evaluated using the Mott single-elastic-scattering cross section corrected for screening in a manner based on a convenient factorization of screening and spin-relativistic effects [4]. The screening corrections for the elastic-scattering cross section are adjusted so as to produce transport cross sections that match with results from exact phase-shift calculations [11,12]. Radiative energy losses (bremsstrahlung production events) are sampled individually along each path segment according to bremsstrahlung cross sections, differential in energy, given in [13]; and secondary knock-on electron production is sampled according to the Møller cross section.

Histories of bremsstrahlung photons are followed according to conventional analog Monte Carlo techniques. Individual photon interactions are sampled based on cross sections [14] for photoelectric absorption, coherent scattering, incoherent scattering and pair (and triplet) production. The histories of all photons and secondary electrons (and positrons) produced in the cascade initiated by the primary electron are followed until they either escape the phantom or fall to an energy below chosen cut-off values. For the calculations reported here, a cut-off energy of 1 keV was chosen for both electron and photon histories. In the case of electrons, a history is terminated also if it cannot reach a phantom boundary (i.e., they are trapped in the phantom) and its energy is below a chosen "trapping" energy. For the present calculations, the trapping energy was chosen to be 1 percent of the incident kinetic energy or 1 keV, whichever was larger. At the termination of any electron history, its energy is deposited according to a procedure which approximately accounts for the residual transport.

## III. Results

The results are based on samples of $10^5$ incident histories in each case. The water phantom was assumed to be a right-circular cylinder with a radius equal to 3 $r_0$ and a height equal to 1.25 $r_0$, where $r_0$ is the electron continuous-slowing-down-approximation (CSDA) range (see, e.g., [8]). Values of $r_0$ are given in Table 1. The cylindrical phantom was assumed to be surrounded by vacuum. Electrons are incident at the center of one of the plane end-faces, with a kinetic energy $T_0$ and at an angle $\alpha$ with respect to the cylinder axis. Thus, the phantom can be considered effectively as a semi-infinite plane

[5]The usually-small departures from straight-line spatial displacements for the path segments are taken into account through an approximate procedure outlined in [4].

slab[6]. The 1.25 $r_0$ depth dimension was divided into 200 equal-sized depth intervals for scoring the energy deposition. Although such fine depth intervals lead to somewhat larger statistical fluctuations, they were chosen in an attempt to provide for adequate resolution if the reference depths of 7, 40, 300 and 1000 mg/cm$^2$ fell in regions where the depth-dose distribution was rapidly changing. However, this selection was not sufficient in all cases, and additional calculations (mostly for $\alpha=89°$ and $T_0 \geq 0.7$ MeV) were done for thinner slabs divided into 200 depth bins to obtain improved resolution.

Each depth-dose distribution was represented by points at the mid-point of the histogram bins and fitted by a curve using least-squares spline techniques [15]. This procedure effectively reduces the effects of statistical fluctuations on the results and allows us to interpolate to the depths of interest. Some examples of the curve fits to the histograms are shown in Fig. 1. On the whole, the procedure in these cases seems to have been successful, with only occasional apparent artifacts (slight bumps or wiggles) in the fitted curves. Possible errors from such occasional fitting artifacts are comparable to the statistical uncertainties in the histogram results, which are no more than about 2 percent when the dose is large enough to be of interest.

The final results for the absorbed dose are summarized in Table 2, which gives at each reference depth the directional personal dose equivalent $H_p(d,\alpha)$, per unit incident electron fluence $\Phi$, for the cases considered. No results are given for $T_0$ of 60 and 50 keV because electrons of those energies do not penetrate to the reference depths, and no attempt was made to obtain accurate results for the very small bremsstrahlung tail. Other than the smoothing in depth for each case as described above, no checks have been made as to the smoothness of the results in $T_0$ or $\alpha$. Although the results given here represent a significant amount of computing effort, they may not be sufficient for reliable interpolation in all variables.

In most cases, systematic uncertainties probably dominate the overall uncertainties in the tabular results[7]. However, such uncertainties - associated with the accuracy of the underlying cross sections and distributions, implementation of sampling algorithms, and approximations inherent in the basic electron Monte Carlo transport model - are difficult to estimate. Based on past experience with such calculations, it seems not unreasonable that systematic uncertainties could be 2 percent, perhaps as large as 5 percent depending on the relative depth, leading one to conservatively estimate an overall uncertainty of about 5 percent (estimated at a level of approximately two standard deviations).

Information of perhaps some related interest are the electron albedos, i.e., the fractions of the incident number and of the incident energy of the electrons that are reflected back through the entrance plane surface of the phantom (assumed here as non re-entrant). Such data indicate the numbers and energies involved if one is concerned with the possible effects of the presence of a scattering medium (e.g., air) instead of vacuum at the interface. The albedo results are given in Table 3. Photon energy albedos for these cases are small (a fraction of 1 percent) and have not been listed. The electron number albedos include contributions from both the primary and secondary electrons, and thus can exceed unity.

---

[6]In the worst case, no more than ~1 percent of the initial electron energy escaped through the sides of the phantom via bremsstrahlung.

[7]However, when the dose per unit fluence in Table 1 is small, say below about 0.003 nSv cm$^2$, the statistical uncertainties can be larger than 10%.

## References


[1] J.L. Chartier, private communication, July (1992).

[2] ICRU, "Measurement of Dose Equivalents from External Photon and Electron Radiations," International Commission on Radiation Units and Measurements Report 47 (1992).

[3] ICRP, "Data for Use in Protection Against External Radiation," ICRP Publication 51 in Annals of the International Commission on Radiation Protection **17** (1987).

[4] S.M. Seltzer, "Electron-Photon Monte Carlo Calculations: The ETRAN Code," Appl. Radiat. Isot. **42**, 917 (1991).

[5] J.A. Halbleib, R.P. Kensek, T.A. Mehlhorn, G.D. Valdez, S.M. Seltzer and M.J. Berger, "ITS Version 3.0: The Integrated TIGER Series of Electron/Photon Transport Codes," Sandia National Laboratories Publication SAND91-1634, March (1992).

[6] L. Landau, " On the Energy Loss of Fast Particles by Ionization," J. Phys. (USSR) **8**, 201 (1944).

[7] S.M. Seltzer, "An Overview of ETRAN Monte Carlo Methods," Chap. 7 in *Monte Carlo Transport of Electrons and Photons* (Eds. T.M. Jenkins, W.R. Nelson and A. Rindi), Plenum Press, New York, p. 153 (1987).

[8] ICRU, "Stopping Powers for Electrons and Positrons," International Commission on Radiation Units and Measurements Report 37 (1984).

[9] O. Blunck and S. Leisegang, "Zum Energieverlust schneller Elektronen in dünnen Schichten," Z. Physik **128**, 500 (1950).

[10] S. Goudsmit and J.L. Saunderson, "Multiple Scattering of Electrons," Phys. Rev. **57**, 24 (1940).

[11] M.E. Riley, "Relativistic, Elastic Electron Scattering from Atoms at Energies Greater than 1 keV," Sandia National Laboratories Report SLA-74-0107 (1974); see also M.E. Riley, C.J. MacCallum and F. Biggs, "Theoretical Electron-Atom Elastic Scattering Cross Sections. Selected Elements, 1 keV to 256 keV," At. Data Nucl. Data Tables **15**, 443 (1975).

[12] M.J. Berger and R. Wang, "Multiple-Scattering Angular Deflections and Energy-Loss Straggling," Chap. 2 in *Monte Carlo Transport of Electrons and Photons* (Eds. T.M. Jenkins, W.R. Nelson and A. Rindi), Plenum Press, New York, p. 21 (1987).

[13] S.M. Seltzer and M.J. Berger, "Bremsstrahlung Energy Spectra from Electrons with Kinetic Energy 1 keV - 10 GeV Incident on Screened Nuclei and Orbital Electrons," At. Data Nucl. Data Tables **35**, 345 (1986).

[14] M.J. Berger and J.H. Hubbell, "XCOM: Photon Cross Sections on a Personal Computer," National Bureau of Standards Report NBSIR 87-3597 (1987).

[15] M.J.D. Powell, "Curve Fitting by Cubic Splines," Atomic Energy Research Establishment (Harwell) Report TP 307 (1967).

Table 1. CSDA ranges $r_o$ in water for initial kinetic energies $T_o$.

| $T_o$ (MeV) | $r_o$ (mg/cm$^2$) |
|---|---|
| 0.05 | 4.320E+00 |
| 0.06 | 5.940E+00 |
| 0.07 | 7.762E+00 |
| 0.08 | 9.773E+00 |
| 0.09 | 1.196E+01 |
| 0.10 | 1.431E+01 |
| 0.20 | 4.487E+01 |
| 0.40 | 1.288E+02 |
| 0.60 | 2.265E+02 |
| 0.70 | 2.778E+02 |
| 0.80 | 3.302E+02 |
| 1.00 | 4.367E+02 |
| 1.50 | 7.075E+02 |
| 2.00 | 9.785E+02 |
| 3.00 | 1.514E+03 |
| 4.00 | 2.037E+03 |
| 7.00 | 3.545E+03 |
| 10.00 | 4.975E+03 |

Table 2. Personal dose equivalents per unit incident fluence, $H_p(d,\alpha)/\Phi$, for electron irradiation of a semi-infinite plane slab of water. The results, extracted from Monte Carlo depth-dose calculations assuming a quality factor of unity, are given in units of nSv cm$^2$ as a function of incident angle $\alpha$ and incident kinetic energy $T_o$. Values of $d/r_o$, where $r_o$ is the CSDA range, are provided as a gauge for the reference depths.

a. $d$ = 7 mg/cm$^2$

| $T_o$ (MeV) | $d/r_o$ | $\alpha$ = 0 | 15 | 30 | 45 | 60 | 75 | 89 |
|---|---|---|---|---|---|---|---|---|
| 0.07 | 0.9018 | 0.198 | 0.169 | 0.101 | 0.0430 | 0.0120 | 0.0016 | 0.0000 |
| 0.08 | 0.7163 | 0.963 | 0.862 | 0.604 | 0.324 | 0.124 | 0.0281 | 0.0006 |
| 0.09 | 0.5853 | 1.546 | 1.423 | 1.091 | 0.664 | 0.299 | 0.0810 | 0.0019 |
| 0.10 | 0.4892 | 1.672 | 1.565 | 1.274 | 0.844 | 0.425 | 0.129 | 0.0033 |
| 0.20 | 0.1560 | 0.825 | 0.861 | 0.914 | 0.870 | 0.613 | 0.245 | 0.0065 |
| 0.40 | 0.0543 | 0.447 | 0.460 | 0.512 | 0.593 | 0.598 | 0.295 | 0.0077 |
| 0.60 | 0.0309 | 0.362 | 0.368 | 0.405 | 0.466 | 0.545 | 0.346 | 0.0095 |
| 0.70 | 0.0252 | 0.350 | 0.359 | 0.387 | 0.446 | 0.530 | 0.357 | 0.0095 |
| 0.80 | 0.0212 | 0.332 | 0.339 | 0.362 | 0.414 | 0.502 | 0.373 | 0.0102 |
| 1.00 | 0.0160 | 0.316 | 0.322 | 0.342 | 0.387 | 0.467 | 0.400 | 0.0110 |
| 1.50 | 0.0099 | 0.293 | 0.296 | 0.311 | 0.342 | 0.410 | 0.439 | 0.0132 |
| 2.00 | 0.0072 | 0.282 | 0.286 | 0.300 | 0.326 | 0.380 | 0.445 | 0.0160 |
| 3.00 | 0.0046 | 0.278 | 0.278 | 0.290 | 0.308 | 0.350 | 0.437 | 0.0219 |
| 4.00 | 0.0034 | 0.275 | 0.281 | 0.284 | 0.302 | 0.334 | 0.428 | 0.0254 |
| 7.00 | 0.0020 | 0.277 | 0.277 | 0.281 | 0.290 | 0.319 | 0.391 | 0.0430 |
| 10.00 | 0.0014 | 0.281 | 0.287 | 0.284 | 0.292 | 0.313 | 0.367 | 0.0601 |

b. $d$ = 40 mg/cm$^2$

| $T_o$ (MeV) | $d/r_o$ | $\alpha$ = 0 | 15 | 30 | 45 | 60 | 75 | 89 |
|---|---|---|---|---|---|---|---|---|
| 0.20 | 0.8913 | 0.0941 | 0.0784 | 0.0453 | 0.0184 | 0.0045 | 0.0007 | 0.0000 |
| 0.40 | 0.3106 | 0.769 | 0.752 | 0.680 | 0.518 | 0.303 | 0.108 | 0.0028 |
| 0.60 | 0.1766 | 0.527 | 0.547 | 0.577 | 0.538 | 0.363 | 0.139 | 0.0036 |
| 0.70 | 0.1440 | 0.476 | 0.495 | 0.535 | 0.528 | 0.378 | 0.150 | 0.0038 |
| 0.80 | 0.1211 | 0.428 | 0.445 | 0.498 | 0.525 | 0.399 | 0.160 | 0.0039 |
| 1.00 | 0.0916 | 0.380 | 0.397 | 0.443 | 0.499 | 0.423 | 0.179 | 0.0043 |
| 1.50 | 0.0565 | 0.326 | 0.337 | 0.368 | 0.434 | 0.464 | 0.231 | 0.0051 |
| 2.00 | 0.0409 | 0.310 | 0.315 | 0.335 | 0.390 | 0.464 | 0.276 | 0.0062 |
| 3.00 | 0.0264 | 0.292 | 0.297 | 0.308 | 0.343 | 0.425 | 0.369 | 0.0083 |
| 4.00 | 0.0196 | 0.288 | 0.290 | 0.299 | 0.325 | 0.396 | 0.420 | 0.0101 |
| 7.00 | 0.0113 | 0.286 | 0.287 | 0.291 | 0.306 | 0.345 | 0.455 | 0.0163 |
| 10.00 | 0.0080 | 0.287 | 0.291 | 0.291 | 0.299 | 0.327 | 0.440 | 0.0223 |

Table 2. (Continued)

c. $d = 300$ mg/cm$^2$

| $T_o$ (MeV) | $d/r_o$ | $\alpha = 0$ | 15 | 30 | 45 | 60 | 75 | 89 |
|---|---|---|---|---|---|---|---|---|
| 0.70 | 1.0799 | 0.0001 | 0.0002 | 0.0001 | 0.0000 | 0.0000 | 0.0000 | 0.0000 |
| 0.80 | 0.9085 | 0.0347 | 0.0283 | 0.0150 | 0.0055 | 0.0011 | 0.0001 | 0.0000 |
| 1.00 | 0.6870 | 0.314 | 0.282 | 0.198 | 0.105 | 0.0394 | 0.0081 | 0.0001 |
| 1.50 | 0.4240 | 0.530 | 0.505 | 0.420 | 0.290 | 0.149 | 0.0450 | 0.0009 |
| 2.00 | 0.3066 | 0.477 | 0.480 | 0.455 | 0.359 | 0.205 | 0.0688 | 0.0014 |
| 3.00 | 0.1982 | 0.374 | 0.389 | 0.420 | 0.418 | 0.289 | 0.106 | 0.0020 |
| 4.00 | 0.1473 | 0.336 | 0.344 | 0.378 | 0.423 | 0.350 | 0.138 | 0.0027 |
| 7.00 | 0.0846 | 0.312 | 0.315 | 0.325 | 0.364 | 0.429 | 0.240 | 0.0044 |
| 10.00 | 0.0603 | 0.310 | 0.310 | 0.317 | 0.336 | 0.409 | 0.321 | 0.0061 |

d. $d = 1000$ mg/cm$^2$

| $T_o$ (MeV) | $d/r_o$ | $\alpha = 0$ | 15 | 30 | 45 | 60 | 75 | 89 |
|---|---|---|---|---|---|---|---|---|
| 2.00 | 1.0219 | 0.0020 | 0.0016 | 0.0007 | 0.0002 | 0.0001 | 0.0000 | 0.0000 |
| 3.00 | 0.6605 | 0.343 | 0.310 | 0.220 | 0.115 | 0.0399 | 0.0073 | 0.0001 |
| 4.00 | 0.4909 | 0.453 | 0.431 | 0.359 | 0.233 | 0.106 | 0.0265 | 0.0004 |
| 7.00 | 0.2821 | 0.361 | 0.372 | 0.398 | 0.379 | 0.237 | 0.0739 | 0.0012 |
| 10.00 | 0.2010 | 0.335 | 0.338 | 0.358 | 0.400 | 0.335 | 0.118 | 0.0019 |

Table 3. Electron number and energy albedos. The results give the fraction of the incident number and of the incident energy, respectively, of electrons that are reflected back through the entrance plane of a semi-infinite slab water phantom, as functions of the incident angle $\alpha$ and the incident kinetic energy $T_o$. The results pertain to electrons backscattered with energies above the cut-off of 1 keV.

Electron energy albedo

| $T_o$ (MeV) | $\alpha$ = 0 | 15 | 30 | 45 | 60 | 75 | 89 |
|---|---|---|---|---|---|---|---|
| 0.05 | 0.029 | 0.034 | 0.050 | 0.088 | 0.169 | 0.336 | 0.715 |
| 0.06 | 0.029 | 0.033 | 0.050 | 0.088 | 0.169 | 0.337 | 0.716 |
| 0.07 | 0.027 | 0.031 | 0.047 | 0.085 | 0.165 | 0.333 | 0.715 |
| 0.08 | 0.028 | 0.033 | 0.050 | 0.088 | 0.170 | 0.339 | 0.717 |
| 0.09 | 0.025 | 0.030 | 0.045 | 0.082 | 0.162 | 0.331 | 0.714 |
| 0.10 | 0.026 | 0.031 | 0.046 | 0.084 | 0.165 | 0.334 | 0.716 |
| 0.20 | 0.023 | 0.027 | 0.043 | 0.081 | 0.161 | 0.331 | 0.717 |
| 0.40 | 0.018 | 0.022 | 0.037 | 0.072 | 0.150 | 0.320 | 0.717 |
| 0.60 | 0.014 | 0.017 | 0.030 | 0.062 | 0.137 | 0.308 | 0.715 |
| 0.70 | 0.014 | 0.017 | 0.030 | 0.063 | 0.138 | 0.309 | 0.717 |
| 0.80 | 0.012 | 0.016 | 0.028 | 0.059 | 0.133 | 0.302 | 0.724 |
| 1.00 | 0.010 | 0.013 | 0.025 | 0.054 | 0.125 | 0.295 | 0.731 |
| 1.50 | 0.0065 | 0.0084 | 0.017 | 0.042 | 0.106 | 0.270 | 0.742 |
| 2.00 | 0.0050 | 0.0064 | 0.013 | 0.034 | 0.092 | 0.252 | 0.740 |
| 3.00 | 0.0028 | 0.0037 | 0.0082 | 0.023 | 0.070 | 0.218 | 0.733 |
| 4.00 | 0.0018 | 0.0026 | 0.0056 | 0.017 | 0.058 | 0.198 | 0.728 |
| 7.00 | 0.0006 | 0.0008 | 0.0021 | 0.0076 | 0.033 | 0.147 | 0.703 |
| 10.00 | 0.0004 | 0.0005 | 0.0011 | 0.0040 | 0.021 | 0.117 | 0.688 |

Electron number albedo

| $T_o$ (MeV) | $\alpha$ = 0 | 15 | 30 | 45 | 60 | 75 | 89 |
|---|---|---|---|---|---|---|---|
| 0.05 | 0.055 | 0.063 | 0.092 | 0.154 | 0.269 | 0.467 | 0.799 |
| 0.06 | 0.054 | 0.063 | 0.092 | 0.154 | 0.269 | 0.468 | 0.800 |
| 0.07 | 0.052 | 0.060 | 0.088 | 0.149 | 0.265 | 0.466 | 0.800 |
| 0.08 | 0.054 | 0.062 | 0.092 | 0.154 | 0.271 | 0.472 | 0.803 |
| 0.09 | 0.050 | 0.058 | 0.086 | 0.147 | 0.263 | 0.465 | 0.802 |
| 0.10 | 0.051 | 0.060 | 0.087 | 0.150 | 0.267 | 0.469 | 0.805 |
| 0.20 | 0.047 | 0.056 | 0.085 | 0.150 | 0.267 | 0.471 | 0.812 |
| 0.40 | 0.042 | 0.050 | 0.079 | 0.143 | 0.262 | 0.471 | 0.823 |
| 0.60 | 0.035 | 0.043 | 0.070 | 0.133 | 0.253 | 0.471 | 0.831 |
| 0.70 | 0.035 | 0.043 | 0.072 | 0.134 | 0.255 | 0.474 | 0.835 |
| 0.80 | 0.033 | 0.040 | 0.068 | 0.129 | 0.253 | 0.472 | 0.849 |
| 1.00 | 0.029 | 0.036 | 0.063 | 0.123 | 0.246 | 0.470 | 0.862 |
| 1.50 | 0.021 | 0.026 | 0.050 | 0.107 | 0.228 | 0.459 | 0.896 |
| 2.00 | 0.017 | 0.022 | 0.042 | 0.095 | 0.215 | 0.454 | 0.913 |
| 3.00 | 0.012 | 0.015 | 0.031 | 0.075 | 0.186 | 0.430 | 0.949 |
| 4.00 | 0.0090 | 0.012 | 0.024 | 0.063 | 0.170 | 0.423 | 0.975 |
| 7.00 | 0.0057 | 0.0072 | 0.014 | 0.040 | 0.128 | 0.389 | 1.052 |
| 10.00 | 0.0047 | 0.0059 | 0.011 | 0.029 | 0.103 | 0.364 | 1.121 |

**Figure Caption**

Fig. 1. Illustration of curves fitted to the calculated histograms of the depth-dose distributions. The results give the scaled, dimensionless absorbed dose, per unit incident current, as a function of depth $z$ (expressed as fractions of the CSDA range $r_o$) for 3-MeV electrons incident on a semi-infinite plane slab of water, at the incident angles $\alpha$ considered here. Vertical lines merely indicate the abscissa values corresponding to the reference depths of 7, 40, 300 and 1000 mg/cm$^2$, and are not error bars. Absorbed dose per unit incident current can be converted to absorbed dose per unit incident fluence through multiplication by cos$\alpha$.

a. $\alpha = 0°$
b. $\alpha = 15°$
c. $\alpha = 30°$
d. $\alpha = 45°$
e. $\alpha = 60°$
f. $\alpha = 75°$
g. $\alpha = 89°$

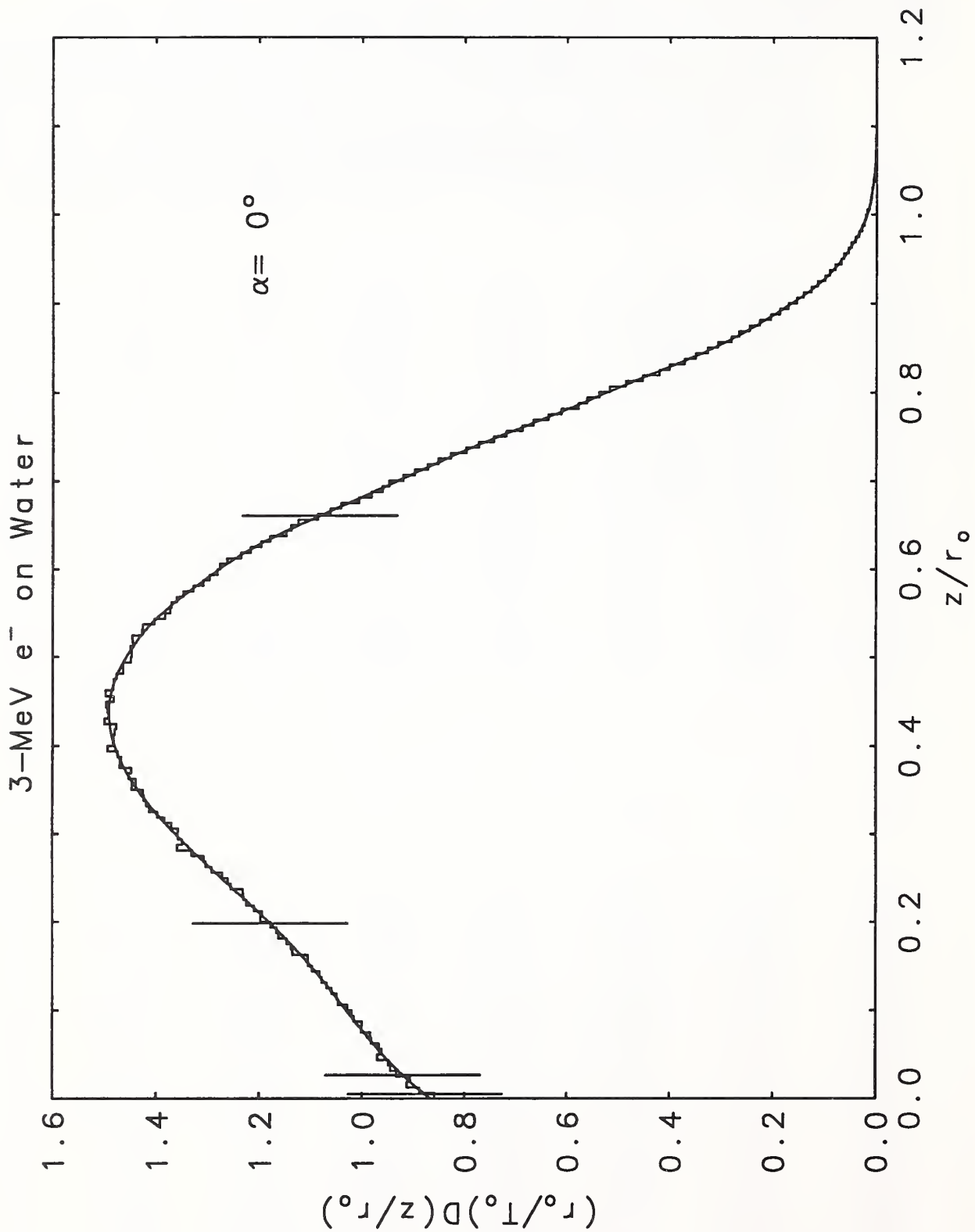


Fig. 1a

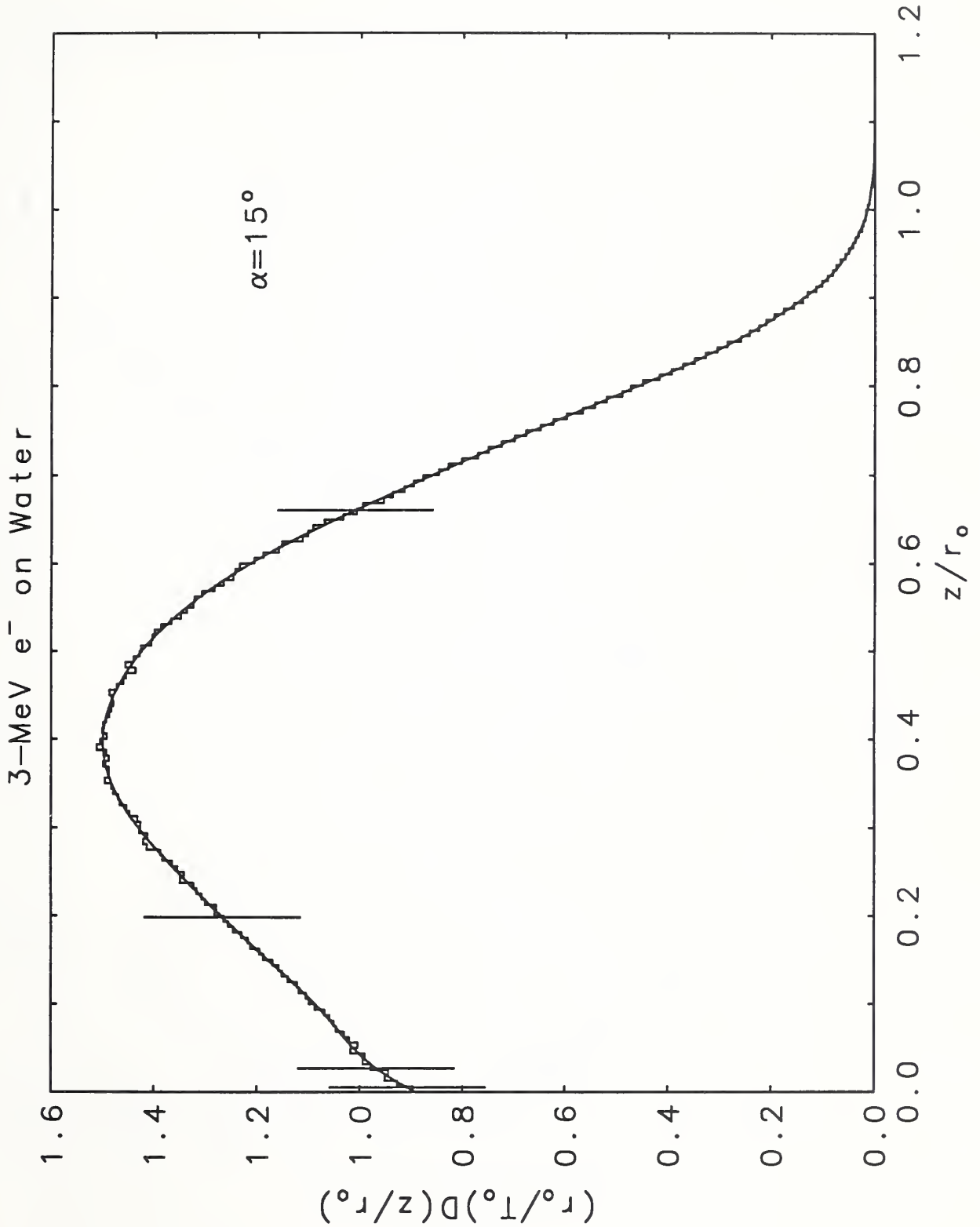


Fig. 1b

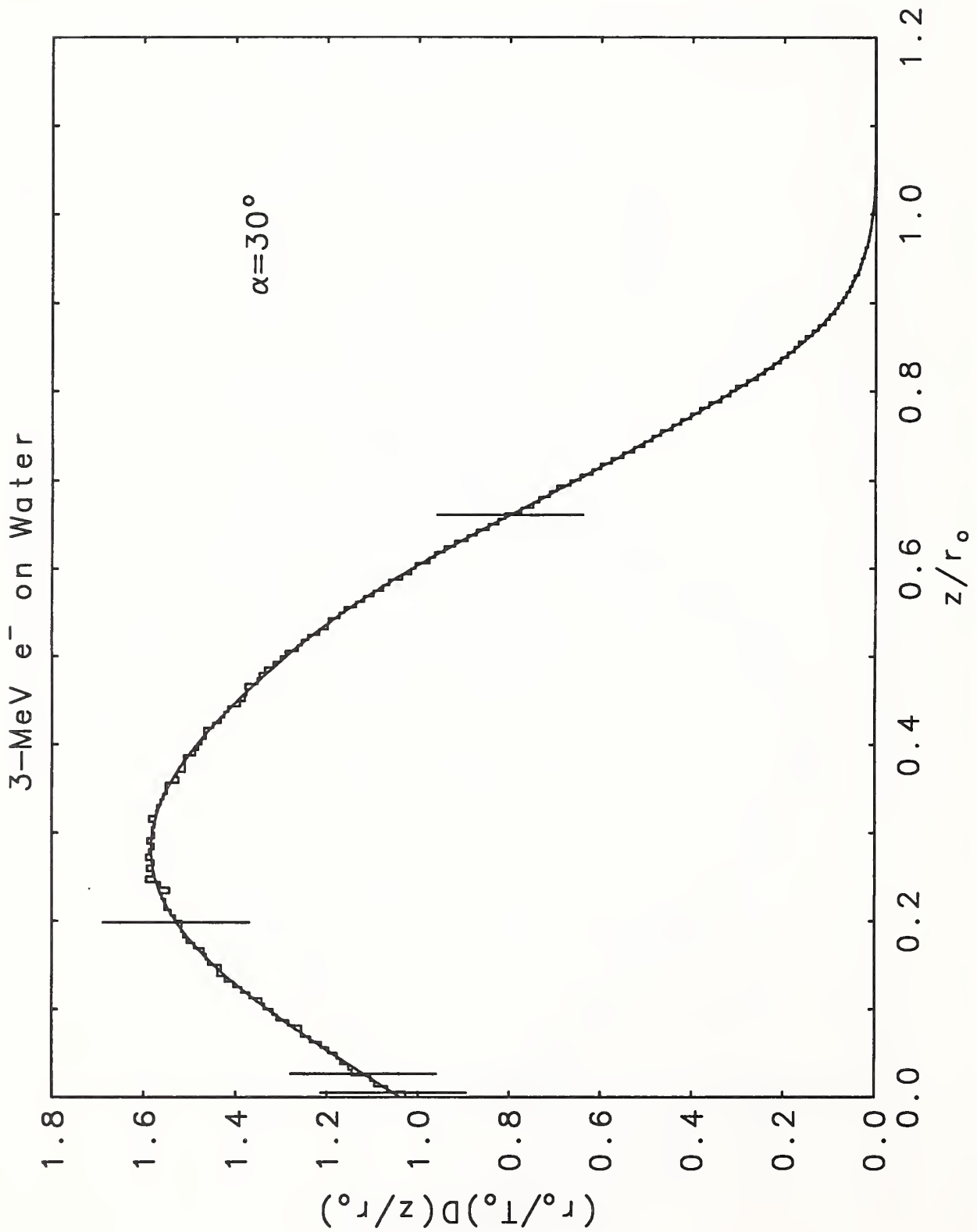


Fig. 1c

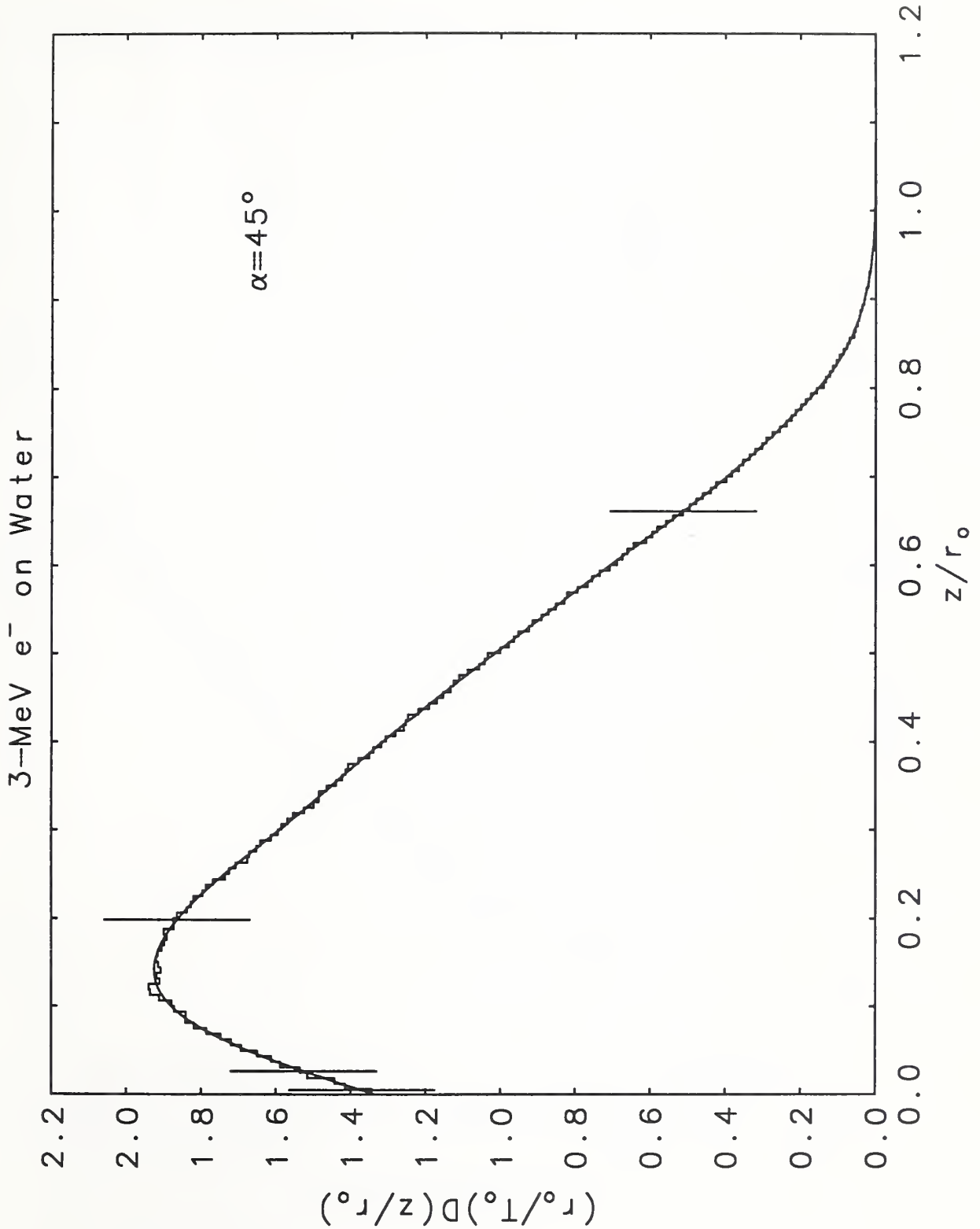


Fig. 1d

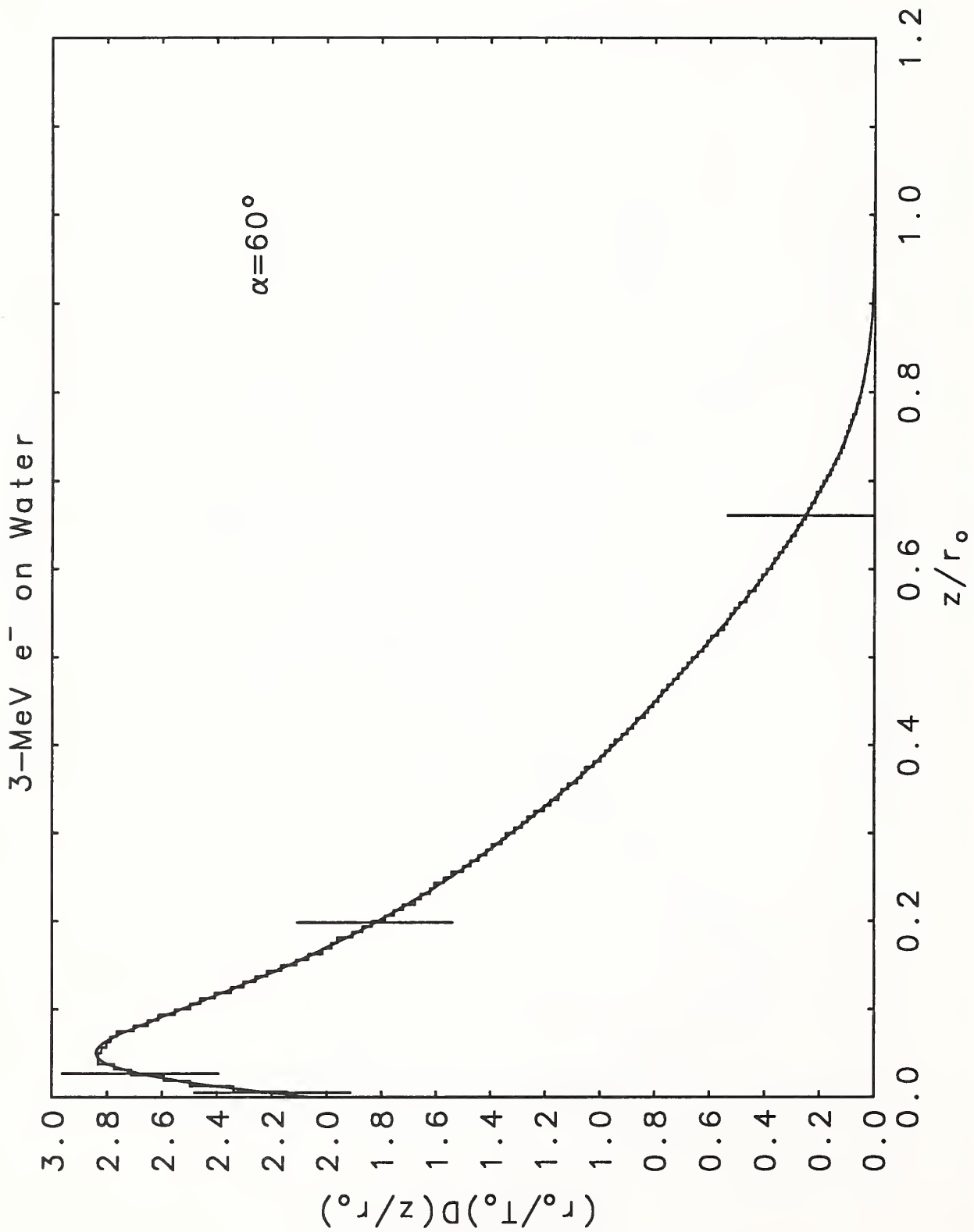
3-MeV e⁻ on Water
α=60°
(r°/T°)D(z/r°)
z/r°
0.0
0.2
0.4
0.6
0.8
1.0
1.2
0.0
0.2
0.4
0.6
0.8
1.0
1.2
1.4
1.6
1.8
2.0
2.2
2.4
2.6
2.8
3.0

Fig. 1e

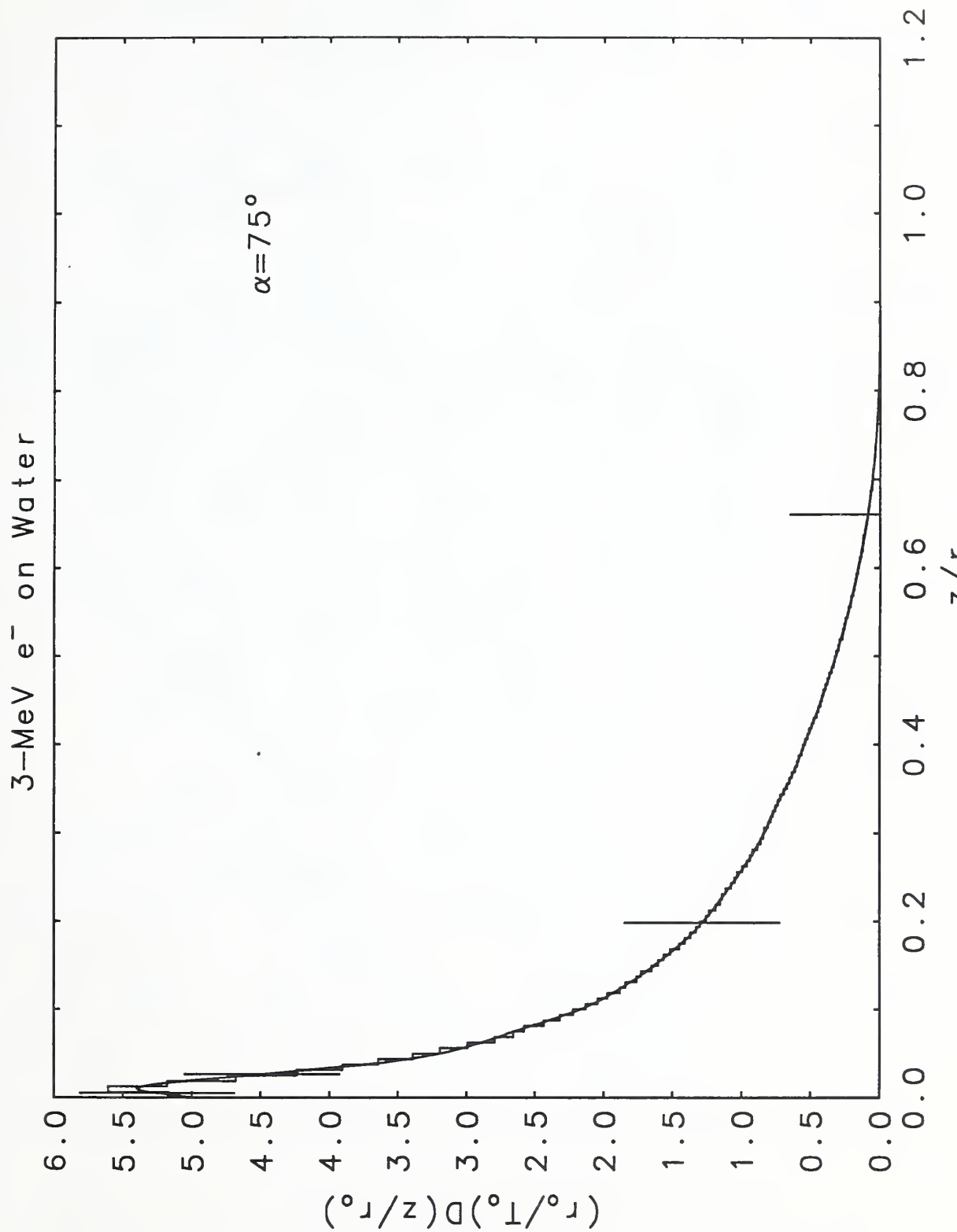
3-MeV e⁻ on Water
α=75°
(r₀/T₀)D(z/r₀)
z/r₀
0.0
0.5
1.0
1.5
2.0
2.5
3.0
3.5
4.0
4.5
5.0
5.5
6.0
0.0
0.2
0.4
0.6
0.8
1.0
1.2

Fig. 1f

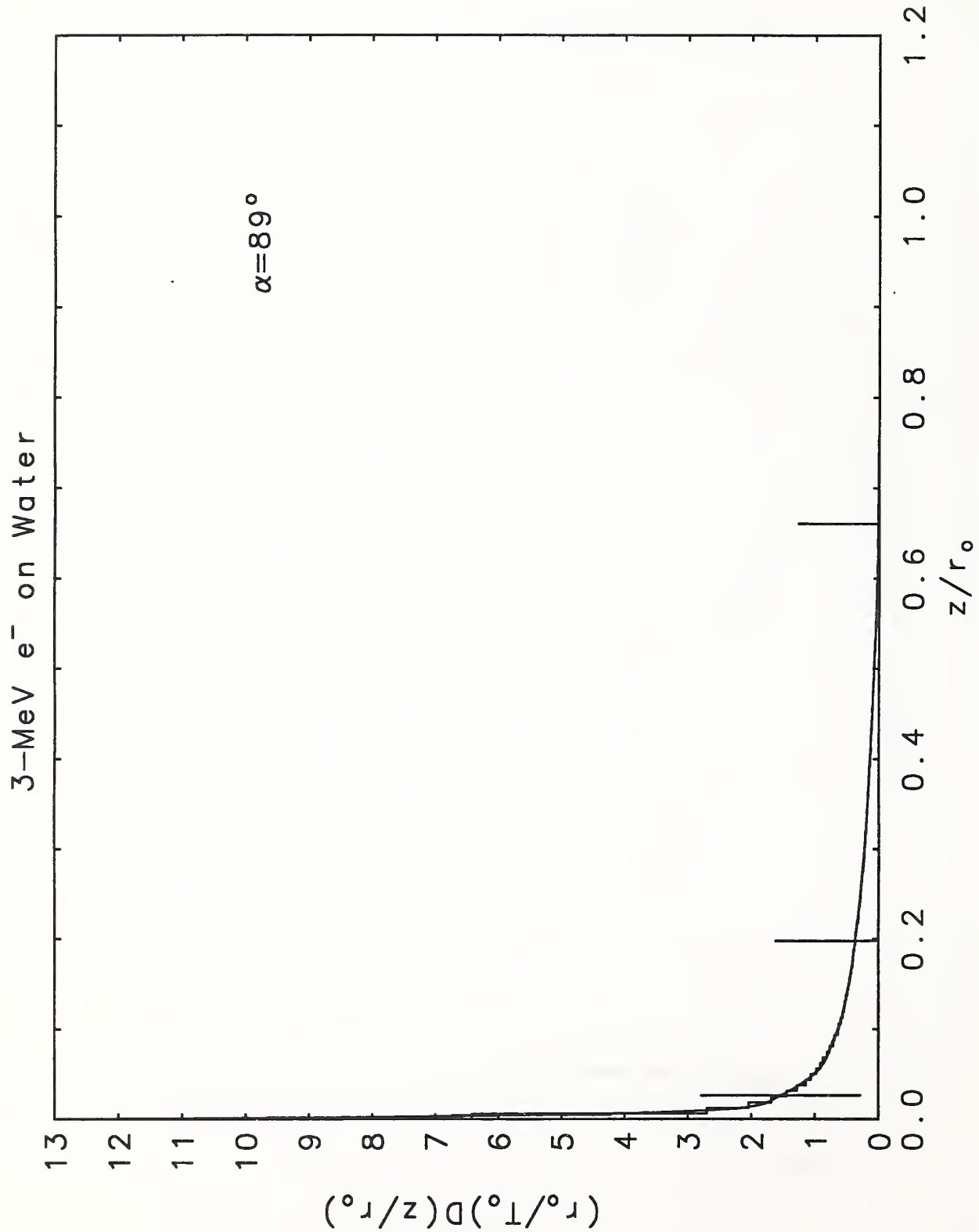
3–MeV e⁻ on Water
α=89°
(r°/T°)D(z/r°)
z/r°
0
1
2
3
4
5
6
7
8
9
10
11
12
13
0.0
0.2
0.4
0.6
0.8
1.0
1.2

Fig. 1g